


Total dose effect of Al_2O_3 -based metal–oxide–semiconductor structures and its mechanism under gamma-ray irradiation

H P Zhu^{1,2} , Z S Zheng^{1,2,5}, B Li^{1,2,5}, B H Li^{1,2}, G P Zhang³, D L Li¹, J T Gao¹, L Yang^{1,2}, Y Cui^{1,2}, C P Liang¹, J J Luo^{1,2} and Z S Han^{1,2,4}

¹Institute of Microelectronics, Chinese Academy of Sciences, Beijing 100029, People's Republic of China

²Key Laboratory of Silicon Device Technology, Chinese Academy of Sciences, Beijing 100029, People's Republic of China

³Department of Physics, Indiana State University, Terre Haute, IN 47809, United States of America

⁴University of Chinese Academy of Sciences, Beijing 100049, People's Republic of China

E-mail: zhengzhongshan@ime.ac.cn and libo3@ime.ac.cn

Received 3 July 2018

Accepted for publication 15 August 2018

Published 11 October 2018



Abstract

In our work, insights into the total dose response and native point defect behavior in the Al_2O_3 gate dielectric during irradiation were gained by gamma-ray irradiation experiments and first-principles calculations. It is found that the O vacancy (V_O) can act as a hole trap in the Al_2O_3 gate dielectric during irradiation, leading to the negative shift of the capacitance–voltage ($C-V$) curves of the Al_2O_3 -based metal–oxide–semiconductor (MOS) structure. Our calculations show that the neutral defect V_O becomes a +2 charged center after irradiation, and the positively charged V_O is a kind of conductive path for electrons, which contributes to an increase of the leakage current in the irradiated MOS capacitors. Additionally, the trapped holes are accumulated with irradiation doses, which can lower the barrier height of the Al_2O_3 gate oxide and further cause the increase of the leakage current. The other native point defects in the Al_2O_3 layer, such as aluminum vacancy (V_{Al}), aluminum interstitial (Al_i) and oxygen interstitial (O_i), only act as fixed charge centers during irradiation. Net negative charges existing in the Al_2O_3 layers before irradiation are mainly induced by the negatively charged defects of V_{Al} and O_i .

Supplementary material for this article is available [online](#)

Keywords: total dose effect, first-principles calculations, native point defects, oxide traps, leakage current

(Some figures may appear in colour only in the online journal)

1. Introduction

As a kind of high κ gate materials, Al_2O_3 dielectric has attracted great interest due to its excellent characteristics, such as a higher crystallization temperature [1], wider band gap [2] and lower interface state density [3], compared to other high κ gate dielectrics, and it has extensive potential applications in advanced microelectronic technologies [4–11]. When considering the radiation tolerance of the advanced

microelectronic devices operating under total dose radiation environments, however, the total dose effect of the Al_2O_3 dielectric becomes a matter of concern.

Up to now, lots of experimental studies have reported on the effect of radiation on metal–oxide–semiconductor (MOS) devices with an Al_2O_3 gate dielectric [3, 12, 13]. Yilmaz *et al* [12] found that a magnetron sputtering Al_2O_3 dielectric is very sensitive to total dose radiation, and the radiation induced oxide-trapped charges in the tested Al_2O_3 film are about ten times larger than that in thermal SiO_2 . Suria *et al* [3] compared the radiation responses of atomic layer deposited

⁵ Authors to whom any correspondence should be addressed.

(ALD) Al_2O_3 , HfO_2 and thermal SiO_2 , and the results suggested that radiation induced net oxide-trapped charge density in the ALD Al_2O_3 is greater than that in ALD HfO_2 , but lower than that in thermal SiO_2 . Felix *et al* [13] also studied the effect of annealing processes on the radiation resistance of Al_2O_3 - SiO_xN_y dielectrics, and an enhanced radiation hardness was observed for the dielectrics with proper annealing conditions.

As known from the above irradiation experiments [3, 12, 13], charge traps in the Al_2O_3 gate dielectric play an important role in the degradation of the performance of the MOS capacitors. As the charge traps are introduced by native point defects in the Al_2O_3 dielectric, understanding the structural and electronic characteristics of these defects and their impact on the radiation response of the MOS capacitors is necessary so that we can increase the radiation hardness of the Al_2O_3 dielectric by improving growth conditions or annealing processes. First-principles calculations for native point defects in Al_2O_3 have already been reported [14–17], most of these studies, nevertheless, are focused on MOS capacitors based on III–V semiconductors [14–16], and there is still a lack of research on MOS capacitors based on a Si substrate. Consequently, although there are many studies into the total dose response of the Al_2O_3 -based MOS capacitors and the native point defects in the Al_2O_3 material, the radiation mechanism is still unclear.

In order to have an insight into the radiation mechanism, irradiation experiments and density functional theory (DFT) calculations are employed in our work. The radiation response of MOS capacitors and electronic properties of the native point defects in Al_2O_3 gate oxide are discussed in this paper. Our results specify the origin of the oxide traps, and give interpretations for the increase of the leakage current in the irradiated MOS capacitors.

2. Experimental details

A MOS structure composed of $\text{Al}/\text{Al}_2\text{O}_3/\text{Si}$ was used in the irradiation experiments. The Al_2O_3 layer with a thickness of about 19 nm was deposited by thermal ALD on the (001) surface of a p-type single crystal silicon (Si) wafers with a resistivity of 8–12 $\Omega\text{ cm}$, as shown in figure 1. A circular aluminum electrode was sputtered on the top of the Al_2O_3 layer, and its thickness is about 400 nm and its area is about $7.065 \times 10^{-4}\text{ cm}^2$. Finally, the MOS capacitors were annealed in a N_2 and H_2 atmosphere at 400 $^\circ\text{C}$ for 20 min.

The MOS capacitors were irradiated with ^{60}Co γ -rays at room temperature up to 8 Mrad(Si) with a dose rate of 50 rad(Si) s^{-1} . No external bias voltages were applied during irradiation in order to study the intrinsic radiation response of the Al_2O_3 layer. Pre- and post-irradiation capacitance–voltage (C – V) curves with a high frequency of 1 MHz and current density–voltage (J – V) characteristics of the MOS capacitor were obtained, respectively, using a Keithley 4200 semiconductor parameter analyzer. The extracted relative dielectric constant of the Al_2O_3 layer from the C – V curves is about 7.48, which is smaller than the reported one (8.6) [18].

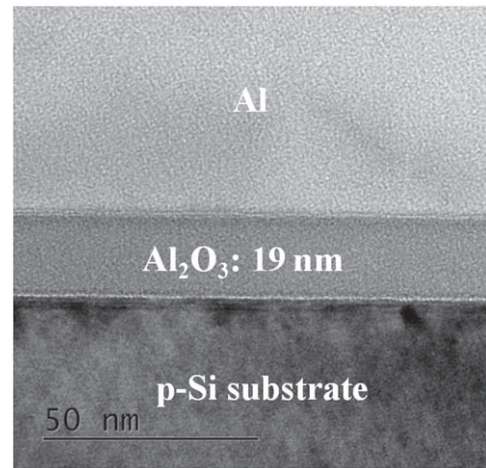


Figure 1. Transmission electron microscope image of an Al_2O_3 -based MOS capacitor.

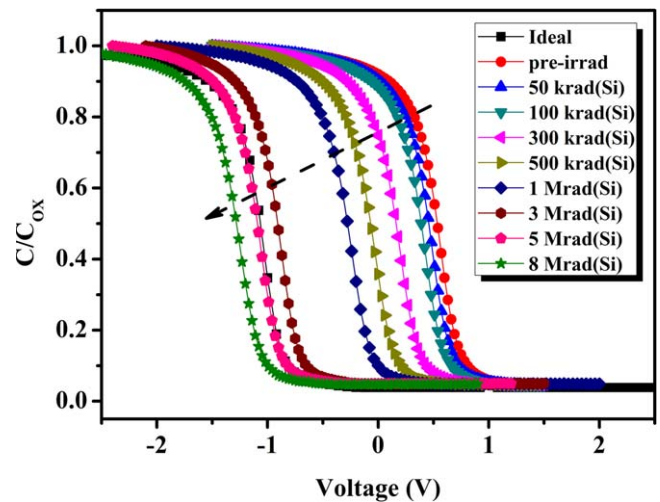


Figure 2. Pre- and post-irradiation capacitance–voltage (C – V) characteristics for the Al_2O_3 -based MOS capacitors along with the ideal C – V curve.

This may be due to a SiO_x interfacial layer which was frequently reported as a byproduct of layer growth via ALD on a Si substrate [18–20].

3. Experimental results and discussions

The measured pre- and post-irradiation C – V characteristics of the MOS capacitors are represented in figure 2 along with the ideal C – V curve. Significantly negative shifts of the C – V curves are observed after irradiation, so holes are trapped by the oxide traps in the Al_2O_3 gate dielectric layer, as reported in [3, 13]. At the same time, it can be observed that there is almost no ‘stretch-out’ in the pre- and post-irradiation C – V curves by comparison with the ideal one. This suggests that there are few interface traps in the pre-irradiated MOS capacitors, and almost no new interface traps are induced by γ -ray irradiation [21]. As a result, radiation has little effect on

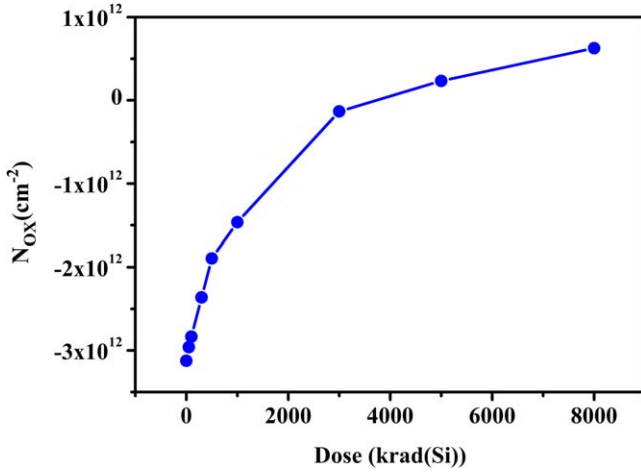


Figure 3. An illustration of the variation of the net charge density N_{ox} for the Al_2O_3 -based MOS capacitors with irradiation dose.

the interface-trapped charges, and the oxide-trapped charges are the main radiation response.

Figure 3 displays net charge density (N_{ox}) in the Al_2O_3 insulator layer as a function of irradiation dose. It can be seen that there is a large amount of net negative charge in the Al_2O_3 gate oxide before irradiation and the corresponding N_{ox} is about $-3.12 \times 10^{12} \text{ cm}^{-2}$. Holes, however, begin to be trapped by the oxide traps during irradiation as discussed above and the number of trapped holes increases as the irradiation dose increases. When the irradiation dose is larger than 3.5 Mrad(Si), a positive value of N_{ox} is obtained as shown in figure 3. This suggests that the number of positive charges induced by irradiation is larger than the number of negative charges in the Al_2O_3 gate layer before irradiation, and thus the net charge density N_{ox} becomes positive.

In order to investigate the radiation effect on the leakage current of the Al_2O_3 dielectric, J - V characteristics were measured, as presented in figure 4(a). The MOS capacitors for the post-irradiation case were irradiated to 8 Mrad(Si). The leakage current density for the post-irradiated MOS capacitors increases strikingly compared with the pre-irradiated one, indicating that the total dose radiation leads to an increase of the leakage current of the Al_2O_3 gate oxide. The mechanism of the leakage current may be attributed to the Poole-Frenkel (PF) effect, since it is usually assigned as the dominating leakage mechanism in metal-insulator-metal thin film stacks [22–25]. The standard quantitative expression for the PF effect is shown as follows [24, 25]

$$J \propto E \exp \left(\frac{-q(\phi_B - \sqrt{qE/(\pi\kappa_d\epsilon_0)})}{k_B T} \right), \quad (1)$$

where J is the current density, and E is the electric field applied on the gate oxide layer, which is the ratio of the difference between the bias voltage and the flat band voltage to the thickness of the gate oxide layer [26]. q is the elementary charge, and ϕ_B is the voltage barrier that an electron (or a hole) escapes from its trap level into the conduction band (or valence band). κ_d represents the self-consistent dynamic dielectric constant, ϵ_0 is the permittivity of vacuum, k_B is

Boltzmann's constant, and T is the temperature. Formula (1) shows that the leakage current is dependent on the temperature T and applied electric field E . Our J - V curve measurements were all carried out at room temperature, so if the leakage current is caused by the PF effect, the plot of the logarithm of J divided by E (namely $\ln(J/E)$) versus the square root of that field E (namely $E^{1/2}$) should be a straight line. Figure 4(b) displays the dependence between $\ln(J/E)$ and $E^{1/2}$ for the pre- and post-irradiation situations, and good linear fits for the leakage of the J - V characteristics are obtained. This implies that the PF effect may be the main leakage mechanism of the Al_2O_3 layer. To further ensure the PF leakage mechanism, dynamic dielectric constants κ_d determined from the slope of the straight lines in figure 4(b) are obtained, as shown in table 1. We can see that both of the κ_d for the pre- and post-irradiation MOS capacitors are close to the previous reported one [27], further revealing that the PF effect is the main leakage mechanism, which is consistent with the other report [26].

Additionally, PF and the Schottky emission (SE) are the two main conduction mechanisms in insulating films and are very similar [28], so to rule out the SE mechanism, dynamic dielectric constants κ_d for the SE are also derived from the slope of the straight lines of $\ln(J)$ as function of $E^{1/2}$. From table 1 we can see that the κ_d for the SE are much smaller than the reported ones [27], suggesting that the SE is not the conduction mechanism of the leakage current in our MOS capacitors.

The PF effect is one of the trap-assisted-tunneling processes, as shown in figure 5(a) [29], and the number of the traps in the Al_2O_3 gate oxide influences the value of the leakage current. As will be shown in the following first-principles calculations, we find that the positively charged oxygen vacancy in the irradiated Al_2O_3 gate oxide becomes a new kind of trap that can induce leakage current. This is one of the reasons for the increase of the leakage current in the post-irradiation MOS capacitors, as observed in figure 4(a).

Another reason for the increase of the leakage current in the Al_2O_3 gate oxide may be the accumulation of the holes trapped in the Al_2O_3 layer during irradiation. As discussed above, before irradiation plenty of net electrons exist in the Al_2O_3 layer, and thus a built-in electric field $\vec{\epsilon}$ is introduced, as displayed in figure 5(b). When a positive bias is applied on the MOS capacitors, an applied electric field \vec{E} is also built in the Al_2O_3 layer. The built-in electric field $\vec{\epsilon}$ has an opposite direction to the applied electric field \vec{E} , so the barrier height of the Al_2O_3 layer is enlarged, as shown in figure 5(b), and the voltage barrier ϕ_B is increased accordingly. Since the voltage barrier ϕ_B is inversely proportional to the current density J as expressed in formula (1), the enhancement of the barrier height will lead to a reduction of the leakage current of the Al_2O_3 insulator layer. For the post-irradiation situation, however, the built-in electric field $\vec{\epsilon}$ becomes smaller, or even has the same the direction with the applied electric field \vec{E} , with the introduction of the trapped holes, so the barrier height of the Al_2O_3 layer is diminished, and the leakage current in the Al_2O_3 insulator layer increases accordingly. For the MOS capacitors exposed to 8 Mrad(Si), the net charges in

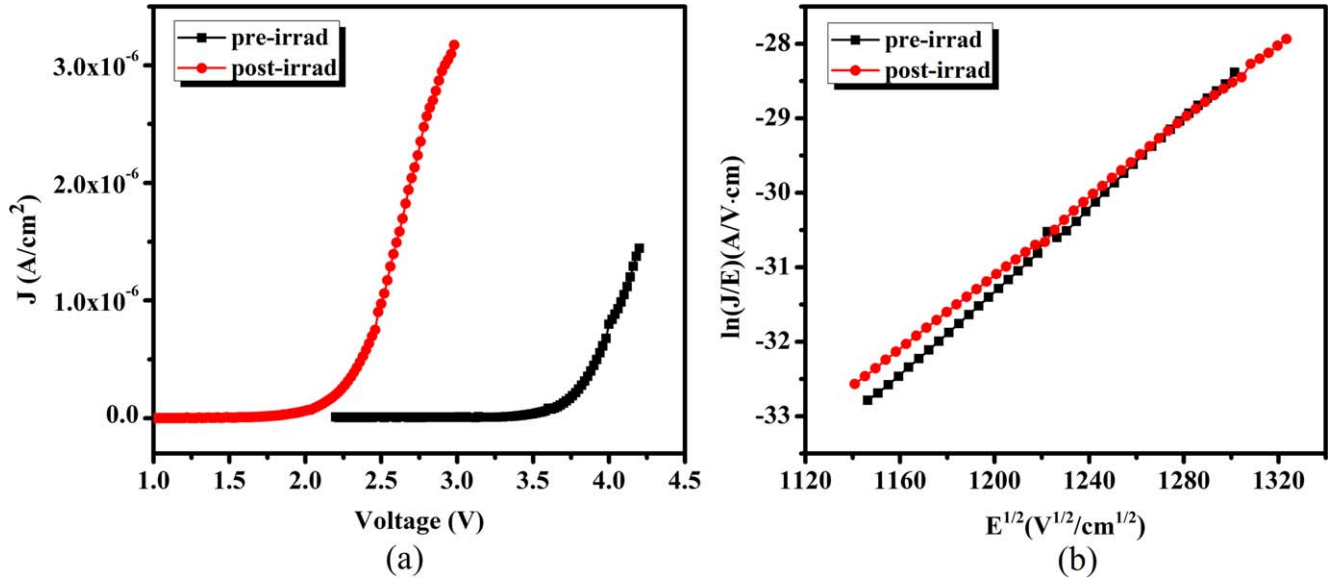


Figure 4. (a) Shows the pre- and post-irradiation current density–voltage (J – V) plots for the Al_2O_3 -based MOS capacitors, where the post-irradiation MOS capacitors were exposed to 8 Mrad(Si). (b) The dependence between the leakage current and the electric field applied on the Al_2O_3 layer for the pre- and post-irradiation MOS capacitors, fitting the PF model.

Table 1. Compare of the dynamic dielectric constants k_d for the pre- and post-irradiation MOS capacitors derived from the PF and Schottky emission (SE) mechanisms.

Type of MOS capacitors	k_d (PF)	k_d (SE)	Conduction mechanism
Pre-irradiation	1.05	0.23	PF
Post-irradiation	1.30	0.29	PF

the Al_2O_3 layer are positive, as shown in figure 3, so the built-in electric field \vec{E} is parallel with the applied electric field \vec{E} , as displayed in figure 5(c), and the barrier height of the Al_2O_3 layer decreases significantly. As a result, a striking increase of the leakage current is observed for the post-irradiation case in figure 4(a).

In conclusion, from the experimental results discussed above we know that the defects in the Al_2O_3 gate dielectric will trap holes during irradiation and cause the degradation of the MOS capacitors. The main leakage mechanism of the Al_2O_3 gate oxide is the PF effect. An increase of the leakage current in the Al_2O_3 insulator is observed after irradiation. This may be due to the introduction of a positively charged oxygen vacancy in the irradiated Al_2O_3 layer, which is a new conductive path, and the buildup of holes trapped in the Al_2O_3 layer, which can cause a decrease of the Al_2O_3 gate oxide barrier height.

4. Calculation methods

In order to have an insight into how intrinsic defects in the Al_2O_3 layers behave during irradiation, first-principles simulations were employed. DFT as implemented in the Vienna Ab-initio Simulation Package [30] was used in the

calculations. The projector augmented wave pseudopotentials were chosen to describe the electron–ion interactions [31] and the generalized gradient approximation was employed as the exchange–correlation potential with the Perdew–Burke–Ernzerhof parameterization method [32]. For the calculations of the electronic structures, the screened hybrid-functional HSE06 [33–35] used for the exchange–correlation term that was employed in order to obtain accurate results. The mixing parameter in HSE06 was set to 40%. The plane-wave basis set is converged using a 500 eV energy cutoff. Ionic positions have been optimized until the Feynman–Hellmann forces acting on ions were less than $0.02 \text{ eV } \text{\AA}^{-1}$.

Al_2O_3 as a gate dielectric is often grown by ALD, forming an amorphous structure. However, Choi *et al* [14] confirmed that the position of defect levels are not strongly dependent on the phases, and the results for the point defects in the crystalline material are also applicable to an amorphous structure. The α - Al_2O_3 was used to do the calculations. The optimized lattice parameters for the perfect α - Al_2O_3 crystal are $a = b = 4.807 \text{ \AA}$ and $c = 13.111 \text{ \AA}$, which are good agreement with the experimental values with $a = b = 4.656 \text{ \AA}$ and $c = 13.140 \text{ \AA}$ [36]. To simulate the defects, a $2 \times 2 \times 1$ Al_2O_3 supercell containing 120 atoms [14, 37] was used in this study. A corresponding k -point Monkhorst–Pack mesh used to sample the three-dimensional Brillouin zone was $3 \times 3 \times 2$. The calculated band gap of the α - Al_2O_3 is about 8.7 eV, in agreement with the experimental value of 8.8 eV [38]. Characteristics of defect formation energy were calculated to research the impact of the native point defects on the radiation response of the Al_2O_3 -based MOS capacitors.

The formation energy of a defect X in charge state q is defined as [39]

$$E_f(X^q) = E_{\text{tot}}(X^q) - E_{\text{tot}}(\text{bulk}) - \sum_i n_i (\mu_i - \mu_{i-\text{bulk}} + \Delta\mu_i) + q(\epsilon_f + E_{\text{VBM}} + \Delta V) \quad (2)$$

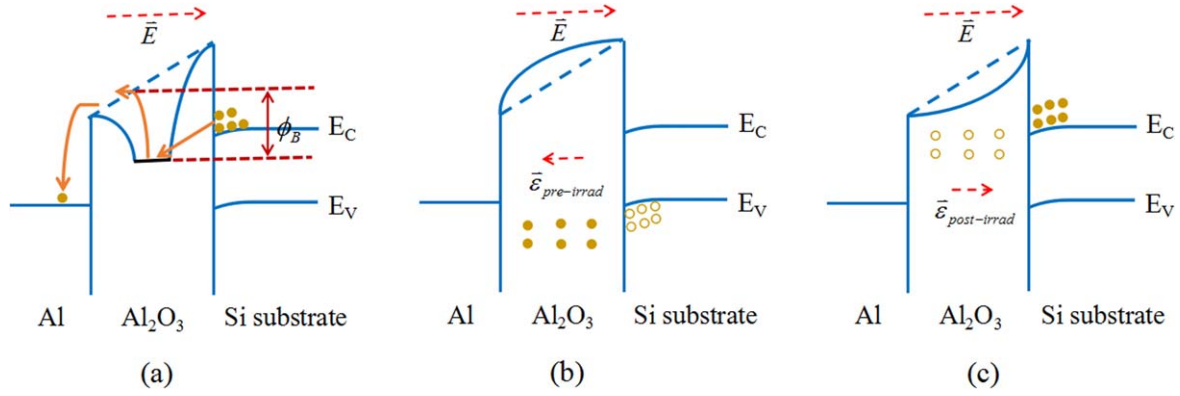


Figure 5. (a) Schematic band diagram of the primary conduction mechanism in the Al_2O_3 dielectric: a PF model; (b) and (c) illustrate the band diagram for the pre- and post-irradiation MOS capacitors with the Al_2O_3 dielectric, respectively. The filled yellow circles represent electrons while the unfilled yellow circles are holes.

where $E_{\text{tot}}(X^q)$ and $E_{\text{tot}}(\text{bulk})$ are the total energies of the X -containing and X -free supercells, respectively; n_i denotes the number of host atoms of species i that have been added to ($n_i > 0$) or removed ($n_i < 0$) from the host when creating the defects. $\mu_{i-\text{bulk}}$ is the chemical potential of species i ($i = \text{Al}$ and O) in solids and, $\Delta\mu_i$ is a relative chemical potential, referenced to $\mu_{i-\text{bulk}}$. q is the charge state of defect X . ε_f is the Fermi level, referenced to the valence band maximum (VBM) of the bulk. Due to the perturbation of the defects, the electrostatic potentials in the defect-containing supercell will change accordingly, and a term ΔV is needed to align the referenced potential in the defect supercell with respect to that in the bulk [40]. In our work, the ΔV was taken as the difference between the electrostatic potentials in the supercell far from the defect and in the Al_2O_3 bulk [40]. $\mu_{\text{Al}-\text{bulk}}$ is equal to the total energy per atom of Al metal and $\mu_{\text{O}-\text{bulk}}$ is equal to the total energy per atom of an isolated O_2 molecule [14].

The chemical potentials $\Delta\mu_{\text{Al}}$ and $\Delta\mu_{\text{O}}$ vary with experimental growth conditions, and in order to maintain the stability of the $\alpha\text{-Al}_2\text{O}_3$ compound, $\Delta\mu_{\text{Al}}$ and $\Delta\mu_{\text{O}}$ must satisfy the condition:

$$2\Delta\mu_{\text{Al}} + 3\Delta\mu_{\text{O}} = \Delta H_f(\text{Al}_2\text{O}_3) \quad (3)$$

where $\Delta H_f(\text{Al}_2\text{O}_3)$ is the formation energy of $\alpha\text{-Al}_2\text{O}_3$ per formula unit. In addition, to avoid precipitation of host atoms of species i under an equilibrium growth condition, the chemical potentials of $\Delta\mu_{\text{Al}}$ and $\Delta\mu_{\text{O}}$ are further limited as:

$$\Delta\mu_{\text{Al}} \leq 0; \quad \Delta\mu_{\text{O}} \leq 0. \quad (4)$$

Thus under an extreme Al-rich condition, $\Delta\mu_{\text{Al}}$ and $\Delta\mu_{\text{O}}$ are equal to 0 and $(1/3)\Delta H_f(\text{Al}_2\text{O}_3)$, respectively, whereas under an extreme O-rich condition, they are equal to $(1/2)\Delta H_f(\text{Al}_2\text{O}_3)$ and 0, respectively.

5. Calculation results and discussions

To have an insight into the total dose effect of the Al_2O_3 dielectric-based MOS capacitors, different types of native

point defects in the Al_2O_3 layer are considered, such as an oxygen vacancy (V_{O}), aluminum vacancy (V_{Al}), oxygen interstitial (O_{i}) and aluminum interstitial (Al_{i}). More details of the defect structures can be seen in the supplementary material, which is available online at stacks.iop.org/SST/33/115010/mmedia. Figure 6 displays the calculated formation energies for these native point defects as a function of the Fermi level ε_f under Al-rich and O-rich conditions, respectively. The slope of an energy line in figure 6 indicates the most stable charge state of the native point defect. It is suggested that the most stable charge state of the intrinsic defects in the Al_2O_3 layer relates to the position of the Fermi level. Taking into account the band alignment between the Al_2O_3 dielectric and the Si semiconductor, the Fermi level of the gate oxide layer is limited in or near the band gap of the Si substrate [41], as shown in the green sections in figure 6. For the unirradiated MOS capacitors, the most stable charge states for the intrinsic defects V_{O} , V_{Al} , O_{i} and Al_{i} , are 0, -3 , -2 and $+3$, respectively, which agree well with other calculation results [14, 42, 43]. The negatively charged defects V_{Al} and O_{i} are responsible for the introduction of the negative charges in the Al_2O_3 layer before irradiation, as observed in figure 3, although a slight compensation happens due to the existence of the positively charged defect Al_{i} .

For semiconductor or insulator materials, the defect levels located below the Fermi level are almost fully occupied by electrons, whereas the defect levels positioned above the Fermi level are almost empty. For a certain defect in the Al_2O_3 dielectric, it may have different charge states accompanied with defect levels lying in different locations in the band gap. If the defect levels for some of the charge states lie below the Fermi level of the Al_2O_3 layer, while other ones for the other charge states are located above the Fermi level, the defect can act as a trap center during irradiation. If the defect levels for all the charge states are all below or above the Fermi level of the Al_2O_3 layer, the corresponding defect behaves as a fixed charge center during irradiation.

Figures 7 and 8 display the locations of the defect levels for the native defects in the Al_2O_3 dielectric, and also show the valence- and conduction-band alignments between the Al_2O_3 dielectric and Si semiconductor [44]. The defect V_{O}

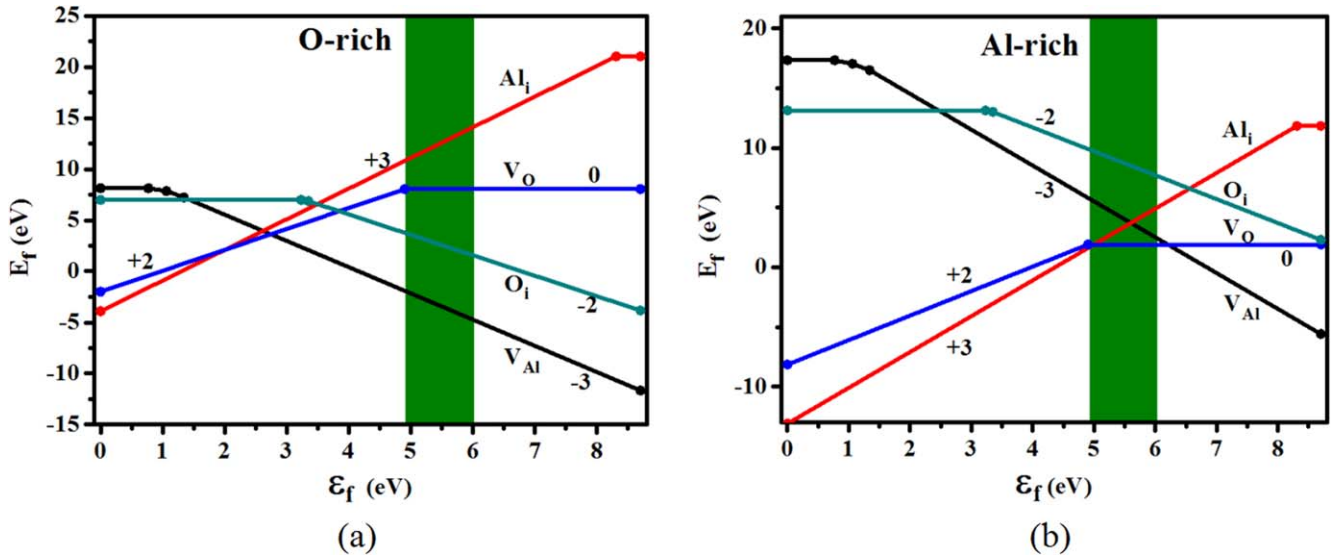


Figure 6. Defect formation energies E_f of the native point defects in the Al_2O_3 gate oxide with the variation of the Fermi level ϵ_f under O-rich (a) and Al-rich (b) conditions. The green colored sections in (a) and (b) correspond to the band gap region of the Si substrate.

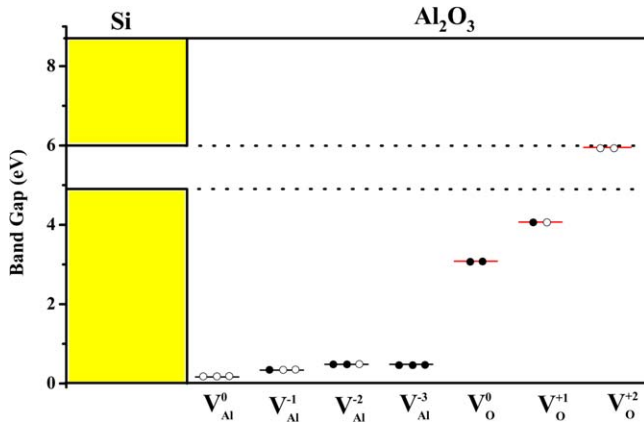


Figure 7. Band offset between the Al_2O_3 gate oxide and Si semiconductor. The defect levels of the aluminum vacancy (V_{Al}) and oxygen vacancy (V_O) are shown with respect to the Si band edges. The filled black circles represent electrons while the unfilled black circles stand for holes.

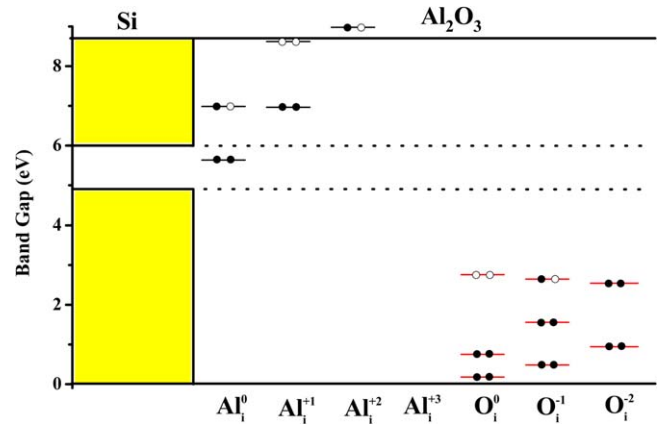


Figure 8. Band offset between the Al_2O_3 gate oxide and Si semiconductor. The defect levels of the aluminum interstitial (Al_i) and oxygen interstitial (O_i) are shown with respect to the Si band edges. The filled black circles represent electrons while the unfilled black circles stand for holes.

has three possible charge states, 0, +1 and +2 in the Al_2O_3 bulk material, and the corresponding defect levels are located about 3.08 eV, 4.07 eV and 5.95 eV above the VBM of the Al_2O_3 , respectively, as displayed in figure 7. The calculated defect positions for the 0 and +1 charged V_O are very close to the experimental results, 3.0 eV and 3.8 eV, as reported in [42, 45–47]. This confirms that our calculated results are accurate and agree well with the experimental results. In the Al_2O_3 -based MOS capacitors, the defect levels for the 0 and +1 charged V_O are all positioned below the VBM of the Si substrate, whereas the defect level for the +2 charged V_O lies just below the conduction band minimum (CBM) of the Si substrate. This suggests that the positions of the 0 and +1 charged defect levels are lower than that of the Fermi level of the Al_2O_3 layer while the position of the +2 charged defect level may be higher than that of the Fermi level of the Al_2O_3 layer. Consequently, V_O may be a trap center. As the most

stable charge state of V_O is 0 before irradiation, it will behave as a hole trap center, and become a +2 charged defect during irradiation, resulting in the negative shift of the $C-V$ curves of the MOS capacitors as observed in figure 2.

From figure 6 we know that the formation energies of V_O are different under different processes. For the O-rich condition, the formation energy of V_O is much bigger than that for the Al-rich condition, suggesting that the number of V_O grown or annealed under an O-rich environment is much fewer, and the radiation hardness of the corresponding MOS capacitors may be much stronger. Felix *et al* [13, 48, 49] have confirmed that the Al_2O_3 -based MOS capacitors with forming gas anneal (FGA) and O_2 anneal have a significantly improved radiation response, and for doses greater than about 1 Mrad (SiO_2), the MOS capacitors with 10 nm and 7.5 nm Al_2O_3 gate oxides annealed with FGA and O_2 anneal have about a 50% less voltage shift than the MOS capacitors with

only a FGA. Thus the radiation hardening may be achieved by additional O_2 anneal.

The defect V_{Al} has four possible charge states 0, -1 , -2 and -3 , in the Al_2O_3 bulk material. However, all the defect levels for the four charge states are deeply located below the VBM of the Si substrate, so the defect level of V_{Al} should be fully occupied by electrons, and cannot capture holes during irradiation. V_{Al} , therefore, is a kind of fixed charge center during irradiation. As discussed above, the most stable charge state of the defect V_{Al} is -3 , so it is a negative fixed charge center.

As for the defect O_i , there are four single degenerate states and three different charge states 0, -1 and -2 . The most stable charge state for O_i in the Al_2O_3 -based MOS capacitor is -2 , and the four defect levels are all occupied by electrons, as displayed in figure 8. As two of the single degenerate defect levels lie deep in the valence band of the Al_2O_3 layer, we do not show them in figure 8. For the -1 and 0 charged O_i , one and two electrons are lost, respectively, and the defect levels shift up correspondingly, but these defect levels are still located below the VBM of the Si substrate and are hard for holes to occupy. The defect O_i , therefore, cannot capture holes during irradiation, and only acts as a negative fixed charge center in the Al_2O_3 gate dielectric.

The defect levels of Al_i are composed of two single degenerate states, as shown in figure 8. The defect Al_i may have four charge states 0, $+1$, $+2$ and $+3$. With the increase of the charge state, the electrons occupied on the defect levels decrease, and the defect levels shift up accordingly, even moving into the conduction band of the Al_2O_3 layer for the $+2$ and $+3$ charge states. As the defect levels for one of the $+2$ charge states and both of the $+3$ charge states lie deep in the conduction band, we do not show them in figure 8. The most stable charge state for Al_i is $+3$. If it could capture electrons during irradiation, the charge state may become $+2$, $+1$, or 0. However, the possibility of the defect levels for $+2$ and $+1$ charged Al_i being occupied by electrons is very small, since these defect levels all lie above the CBM of the Si substrate. As for the 0 charged Al_i , although there is a single degenerate defect level lying in the Si band gap, and it may be occupied by electrons, it is hard for the other single degenerate defect level located above the CBM of the Si substrate to be occupied by electrons. As a result, it is hard for the Al_i to trap electrons during irradiation, and it can only behave as a positively charged center in the Al_2O_3 gate oxide.

From the experimental results, we know that the leakage mechanism of the Al_2O_3 gate insulator layer is trap-assisted tunneling [29]. The electrons tunneling from the cathode are trapped by the capture centers in the gate oxide, then they get into the conduction band of the gate oxide through the PF effect, and finally transport to the anode forming leakage current. Blochl *et al* [50] have reported that whether or not the electrons can transport through the the gate oxide depends on the relationship between the applied voltage and relaxation energy, where the relaxation energy is induced by the change of the defect structure after trapping electrons. Electrons can gain energy under the bias voltage. If the energy is larger than that of the relaxation energy, the electrons can be detrapped

and proceed to the anode, otherwise, they are trapped in the gate oxide [50]. Before irradiation, the charge state of V_O is zero, and its defect level is fully occupied by electrons and located far away from the VBM of the Si substrate, as displayed in figure 7, so it cannot be a conductive path. After irradiation, however, V_O becomes a $+2$ charged trap center, and its defect level is unoccupied by electrons and it lies near the CBM of the Si substrate, so it may be a conductive path in the Al_2O_3 layer. The calculated relaxation energy of the trap center V_O with the charge state changing from $+2$ to $+1$ is about 0.9 eV, demonstrating that the trap center V_O can be conductive with an applied voltage larger than 0.9 V. This calculation result gives an interpretation for the increase of the leakage current in the Al_2O_3 gate oxide after irradiation.

From the above calculation results and discussions, it is known that the intrinsic defect V_O is a trap center, and can capture holes during irradiation, leading to the degeneration of the MOS capacitors. At the same time, the positively charged defect V_O after irradiation is also a kind of conductive path, and it can cause the increase of the leakage current in the Al_2O_3 layer. The other intrinsic defects V_{Al} , Al_i and O_i , are fixed charge centers in the Al_2O_3 gate layer, and cannot capture electrons or holes during irradiation. V_{Al} and O_i are negatively charged centers, and mainly responsible for the introduction of the negative charges in the Al_2O_3 layer.

6. Conclusion

In conclusion, we have investigated the total dose response of the Al_2O_3 -based MOS capacitors and explained the micro-physical mechanism by employing experimental studies and first-principles calculations. It is shown that the native point defects V_O are the hole traps in the Al_2O_3 oxide layer, while the other defects of V_{Al} , Al_i and O_i are fixed charge centers. After irradiation, the $+2$ charged V_O became a conductive path for electrons, resulting in an increase of the leakage current of the Al_2O_3 gate oxide. On the hand, the barrier height of the Al_2O_3 is lowered due to the accumulation of trapped holes during irradiation, which also contributes to the increase of the leakage current. Our study also finds that the negatively charged V_{Al} and O_i are mainly responsible for the net negative charges in the Al_2O_3 layer before irradiation. Our investigation exhibits the total dose response of the Al_2O_3 -based MOS capacitors and gives a basic physical model of the radiation response at an atomic level, which may provide theoretical and experimental support for the study of the radiation-hardened Al_2O_3 gate dielectric.

Acknowledgments

This work was supported by the National Key Research and Development Program of China (2016YFB0901801 and 2016YFB0901804) and by the ‘Era’ of the Computer Network Information Center of the Chinese Academy of Sciences. GPZ was supported by the US Department of Energy under Contract No. DE-FG02-06ER46304. Part of the work

was done on the National Energy Research Scientific Computing Center (NERSC) in the US Department of Energy.

ORCID iDs

H P Zhu  <https://orcid.org/0000-0003-1307-3631>

References

- [1] Jakschik S, Schroeder U, Hecht T, Gutsche M, Seidl H and Bartha J W 2003 *Thin Solid Films* **425** 216
- [2] Afanas'ev V V, Houssa M, Stesmans A, Merckling C, Schram T and Kittl J A 2011 *Appl. Phys. Lett.* **99** 072103
- [3] Suria A J, Chiamori H C, Shankar A and Senesky D G 2015 *Proc. SPIE* **9491** 949105
- [4] Lim D, Lee J H and Choi C 2017 *Microelectron. Eng.* **178** 266
- [5] Chang H Y, Adams B, Chien P Y, Li J and Woo J C S 2013 *IEEE Trans. Electron. Dev.* **60** 92
- [6] Fenouillet-Beranger C et al 2011 *IEEE Int. Conf. on IC Design & Technology (ICICDT)* (<https://doi.org/10.1109/ICICDT.2011.5783186>)
- [7] Liu Y X et al 2014 *ECS Trans.* **61** 263
- [8] Takahashi T, Beppu N, Chen K, Oda S and Uchida K 2011 *International Electron Devices Meeting* (<https://doi.org/10.1109/IEDM.2011.6131672>)
- [9] Wei C Y, Shen B, Ding P, Han P, Li A D, Xia Y D, Xu B, Yin J and Liu Z G 2017 *Sci. Rep.* **7** 5988
- [10] Zhang E, Wang W, Zhang C, Jin Y, Zhu G, Sun Q, Zhang D W, Zhou P and Xiu F 2014 *ACS Nano*. **9** 612
- [11] Raja J, Nguyen C P T, Lee C, Balaji N, Chatterjee S, Jang K, Kim H and Yi J 2016 *IEEE Electron. Device Lett.* **37** 1272
- [12] Yilmaz E, Doğan İ and Turan R 2008 *Nucl. Instrum. Meth. Phys. Res. B* **66** 4896
- [13] Felix J A, Shaneyfelt M R, Fleetwood D M, Schwank J R, Dodd P E, Gusev E P, Fleming R M and D'Emic C 2004 *IEEE Trans. Nucl. Sci.* **51** 3143
- [14] Choi M, Janotti A and Van de Walle C G 2013 *J. Appl. Phys.* **113** 044501
- [15] Weber J R, Janotti A and Van de Walle C G 2009 *Microelectron. Eng.* **86** 1756
- [16] Taylor H D, Lyons J L, Choi M, Janotti A and Van de Walle C G 2015 *J. Vac. Sci. Technol. A* **33** 01A120
- [17] Momida H, Nigo S, Kido G and Ohno T 2011 *Appl. Phys. Lett.* **98** 042102
- [18] Specht M 2003 *33rd European Solid-State Device Research Conference* pp 155–158
- [19] Salomone L S, Kasulin A, Lipovetzky J, Carbonetto S H, Garcia-Inza M A, Redin E G, Berbeglia F, Campabadal F and Faigón A 2014 *J. Appl. Phys.* **116** 174506
- [20] Wilk G D, Wallace R M and Anthony J M 2001 *J. Appl. Phys.* **89** 5243
- [21] Kang A Y, Lenahan P M and Conley J F 2002 *IEEE Trans. Nucl. Sci.* **49** 2636
- [22] Jeong D S and Hwang C S 2005 *J. Appl. Phys.* **98** 113701
- [23] Xu Z, Houssa M, De Gendt S and Heyns M 2002 *Appl. Phys. Lett.* **80** 1975
- [24] Ramesh S, Dutta S, Shankar B and Gopalan S 2015 *Appl. Nanosci.* **5** 115
- [25] Yang W, Marino J, Monson A and Wolden C A 2006 *Semicond. Sci. Technol.* **21** 1573
- [26] Rafi J M et al 2013 *Solid State Electron.* **79** 65
- [27] Ludeke R, Cuberes M T and Cartier E 2000 *Appl. Phys. Lett.* **76** 2886
- [28] Li P and Lu T-M 1991 *Phys. Rev. B* **43** 14261
- [29] Yu S, Guan X and Philip Wong H S 2011 *Appl. Phys. Lett.* **99** 063507
- [30] Kresse G and Furthmüller J 1996 *Phys. Rev. B* **54** 11169
- [31] Kresse G and Joubert D 1999 *Phys. Rev. B* **59** 1758
- [32] Perdew J P, Burke K and Ernzerhof M 1996 *Phys. Rev. Lett.* **77** 3865
- [33] Heyd J, Scuseria G E and Ernzerhof M 2003 *J. Chem. Phys.* **118** 8207
- [34] Heyd J, Scuseria G E and Ernzerhof M 2006 *J. Chem. Phys.* **124** 219906
- [35] Marsman M, Paier J, Stroppa A and Kresse G 2008 *J. Phys.: Condens. Matter* **20** 064201
- [36] d'Amour H, Schiffrer D, Denner W, Schulz H and Holzapfel W B 1978 *J. Appl. Phys.* **49** 4411
- [37] Yang M Y, Kamiya K, Magyari-Köpe B, Momida H, Ohno T, Niwa M, Nishi Y and Shiraishi K 2013 *Jpn. J. Appl. Phys.* **52** 04CD11
- [38] French R H 1990 *J. Am. Ceram. Soc.* **73** 477
- [39] Zhu H P, Gu M Q, Huang L, Wang J L and Wu X S 2014 *Mater. Chem. Phys.* **143** 637
- [40] Van de Walle C G and Neugebauer J 2004 *J. Appl. Phys.* **95** 3851
- [41] Weber J R, Janotti A and Van de Walle C G 2011 *J. Appl. Phys.* **109** 033715
- [42] Matsunaga K, Tanaka T, Yamamoto T and Ikuhara Y 2003 *Phys. Rev. B* **68** 085110
- [43] Hine N D M, Frensch K, Foulkes W M C and Finnis M W 2009 *Phys. Rev. B* **79** 024112
- [44] Robertson J 2000 *J. Vac. Sci. Technol. B* **18** 1785
- [45] Pustovarov V A, Perevalov T V, Gritsenko V A, Smirnova T P and Yelissev A P 2011 *Thin Solid Films* **519** 6319
- [46] Draeger B G and Summer G P 1979 *Phys. Rev. B* **19** 1172
- [47] Surdo A I, Kortov V S, Pustovarov V A and Yakovlev V Y 2005 *Phys. Status Solidi. C* **2** 527
- [48] Felix J A, Shaneyfelt M R, Fleetwood D M, Meisenheimer T L, Schwank J R, Schrimpf R D, Dodd P E, Gusev E P and D'Emic C 2003 *IEEE Trans. Nucl. Sci.* **50** 1910
- [49] Felix J A, Schwank J R, Fleetwood D M, Shaneyfelt M R and Gusev E P 2004 *Microelectron. Reliab.* **44** 563
- [50] Blöchl P E and Stathis J H 1999 *Physica B* **273-274** 1022